

Folding Analytical Devices for Electrochemical ELISA in Hydrophobic R^H Paper

Ana C. Glavan,[†] Dionysios C. Christodouleas,[†] Bobak Mosadegh,[†] Hai Dong Yu,[†] Barbara S. Smith,[†] Joshua Lessing,[†] M. Teresa Fernández-Abedul,^{*,†,§} and George M. Whitesides^{*,†,‡}

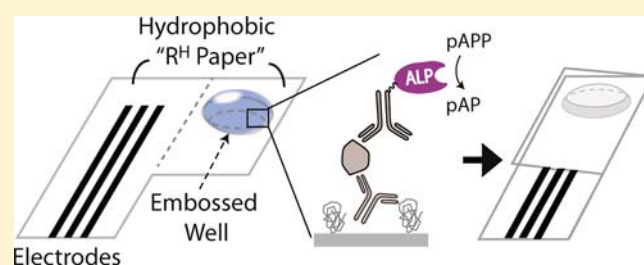
[†]Department of Chemistry and Chemical Biology, Harvard University, Cambridge Massachusetts 01238, United States

[‡]Wyss Institute for Biologically Inspired Engineering, Harvard University, Cambridge, Massachusetts 01238, United States

[§]Departamento de Química Física y Analítica, Universidad de Oviedo, 33006 Oviedo, Asturias, Spain

S Supporting Information

ABSTRACT: This work describes a device for electrochemical enzyme-linked immunosorbent assay (ELISA) designed for low-resource settings and diagnostics at the point of care. The device is fabricated entirely in hydrophobic paper, produced by silanization of paper with decyl trichlorosilane, and comprises two zones separated by a central crease: an embossed microwell, on the surface of which the antigen or antibody immobilization and recognition events occur, and a detection zone where the electrodes are printed. The two zones are brought in contact by folding the device along this central crease; the analytical signal is recorded from the folded configuration. Two proof-of-concept applications, an electrochemical direct ELISA for the detection of rabbit IgG as a model antigen in buffer and an electrochemical sandwich ELISA for the detection of malarial histidine-rich protein from *Plasmodium falciparum* (*Pf* HRP2) in spiked human serum, show the versatility of this device. The limit of detection of the electrochemical sandwich ELISA for the quantification of *Pf* HRP2 in spiked human serum was 4 ng mL⁻¹ (10² pmol L⁻¹), a value within the range of clinically relevant concentrations.



Electrochemical enzyme-linked immunosorbent assay (ELISA) has the potential to be a useful alternative to conventional colorimetric ELISA for clinical diagnostics because the measured analytical signal is insensitive to color interference and can be converted into a numeric output using inexpensive electronics.^{1,2} Typically, electrochemical ELISA is carried out in standard microtiter plates, with the electroactive product of the enzymatic reaction being transferred at the end to an electrochemical cell to perform the readout.²⁻⁴ The complexity of the procedure generally limits electrochemical ELISA to well-resourced laboratories with skilled personnel. Easy-to-use, inexpensive, and reliable devices for electrochemical ELISA that can be mass-produced and that are simple enough to be used, with further development, at the point of care, e.g., in the field, in a patient's home, or in a doctor's office, would be highly desirable, but they are still not widely available. We wished to develop a device for electrochemical ELISA on paper to provide a foundation for the development of low-cost, fieldable devices for resource-limited settings.

Here, we describe the successful fabrication and use of a new, simple family of paper electrochemical devices that can be used for electrochemical ELISA. The devices are made entirely from a sheet of C₁₀^H paper⁵ (cellulose paper that has been rendered hydrophobic by vapor-phase silanization with decyl trichlorosilane) and ink, using only embossing, printing, and folding as techniques for fabrication. Despite the remarkable simplicity of these devices (simplicity in the materials used, the fabrication

method, and the operation) they are highly sensitive and exhibit the electrochemical behavior typical of conventional electrochemical cells.

A number of research programs have focused on the development of devices for electrochemical immunoassays.⁶⁻¹¹ In electrochemical immunosensors, the layers of immobilized antigens and antibodies are attached to the surface of the electrochemical transducers.^{6,12-16} One consequence of this design is that the immobilization of assay species on the surface of the sensor and the sequential incubation and washing steps may cause fouling of the electrodes and may impede electron transfer.¹⁷⁻¹⁹ To limit this potential problem, spatial separation of the immunoreactor and electrochemical detector has been suitable in many cases.^{8,12,20} Aguilar et al.⁷ reported an immunoassay format in which a recessed microdisk (for capturing antigen) and a nanoband gold electrode (for detection) were placed in close proximity within a microcavity. Bhimji et al.⁸ developed an electrochemical ELISA in which the capture and recognition of the antibody occur in close proximity to large, three-dimensional gold microelectrodes. The devices used in these assays are highly sensitive, but they still suffer from drawbacks associated with complex micro-

Received: June 5, 2014

Accepted: November 6, 2014

Published: November 6, 2014



fabrication procedures (e.g., photolithography, thin-film deposition, etching, or bonding),²¹ the use of materials (silicon, glass, or polymers) that are not inexpensive, and the requirement for external reference and auxiliary electrodes.

In recent years, paper has become an attractive material for the fabrication of diagnostic devices for use in the developed and developing world.^{22–26} Micro paper-based analytical devices (μ PADs),^{27–35} have been used, in conjunction with colorimetric,³⁶ fluorescent,³⁷ chemiluminescent,³⁸ and electrochemical^{19,32,39,40} detection technologies, for a variety of applications in bioanalysis, including ELISA.^{36,41} In electrochemical microfluidic paper-based analytical devices (E μ PADs),^{39,42,43} first developed by Henry et al.,³² the porous matrix of cellulose fibers through which analytes must travel to the surface of the electrodes limits convective mass transport.⁴⁴ Indeed, Crooks et al. recently demonstrated that the removal of cellulose fibers from a microfluidic channel in paper, to allow electrodes to contact the solution in the cavity directly, resulted in improved mass transfer within the electroanalytical device.⁴⁴ On the basis of the same principle, cellulose paper that has been rendered hydrophobic can be used to fabricate electrochemical devices that exhibit rapid mass transfer: aqueous droplets can rest directly on the surface of the electrodes printed on hydrophobic paper and form a well-defined electrode–electrolyte interface that enables rapid mass transfer to the surface of the electrode.

C₁₀H paper⁵ (cellulose paper that has been rendered hydrophobic by vapor-phase silanization with decyl trichlorosilane) has several other properties that make it an attractive substrate for the fabrication of devices for electrochemical ELISA: (i) Its low surface free energy allows the printing of electrodes with high reproducibility.⁴⁵ (ii) Its hydrophobicity and high surface area facilitates the immobilization of the capture biomolecules (antibodies and antigens) on its surface. (iii) Its flexibility allows the fabrication of microtiter wells by embossing. (iv) Its foldability allows its use as a substrate for devices with tunable geometry. (v) Its low cost and light weight make it a useful material for the fabrication of disposable devices.

The hydrophobic paper-based device for electrochemical ELISA that we have developed comprises two zones separated by a central crease: an embossed microwell, on the surface of which the antigen immobilization and recognition events occur, and a detection zone where the electrodes are printed. The tunable geometry of the device allowed us to form an electrochemical cell in which the solution of electroactive species contacts the electrodes in the final step of the ELISA: the two zones are brought into contact by folding the device along the central crease, at which point when the analytical signal is recorded. This approach of assembling a device by folding components into contact has also been exploited, by Crooks^{37,46,47} and others,¹⁹ as a means to fabricate paper-based analytical devices. Here, the folding of the device is not just a part of the fabrication process but a step in the analytical assay. It allows us to minimize the fouling of the electrodes and increase the sensitivity of the assay.

As a proof-of-concept demonstration, we used the device for an electrochemical direct ELISA⁴⁸ using rabbit IgG as a model antigen and alkaline phosphatase-labeled anti-rabbit IgG as a model antibody. Once the method was optimized, we used the device to perform an electrochemical direct sandwich⁴⁹ ELISA for the quantification of a clinically relevant antigen, the malarial histidine-rich protein from *Plasmodium falciparum* (Pf

HRP2), spiked into human serum. This article focuses solely on the electrochemical aspects of a demonstration of principle and is not intended to demonstrate a completely prototyped system (including methods for sample preparation and addition).

■ EXPERIMENTAL SECTION

Materials and Chemicals. Chromatography paper (Whatman #1 Chr) was purchased from GE Healthcare (NJ, USA). Graphite ink was prepared by mixing graphite paste (C10903P14 carbon/graphite ink, Gwent Electronic Materials Ltd., Torfaen, UK) and solvent (Ercon N-160 solvent thinner, Ercon Inc., Wareham, MA, USA) in 55:45 m/m ratio. Decyl trichlorosilane was purchased from Gelest Inc. (Morrisville, PA, USA). *p*-aminophenyl phosphate (pAPP) was purchased from Gold Biotechnology (St. Louis, MO, USA). Polystyrene microtiter plates (UltraCruz ELISA Plate, high binding, 96 well, flat bottom) were purchased from Santa Cruz Biotech (Dallas, TX, USA). Rabbit IgG, goat anti-rabbit IgG antibody (A3689), goat anti-rabbit antibody conjugated with alkaline phosphatase (ALP anti-rabbit IgG), ferrocenecarboxylic acid (FCA), bovine serum albumin (BSA) solution (10% m/m in DPBS), human serum, *p*-aminophenol (pAP), alkaline phosphatase yellow (*p*-nitrophenyl phosphate, pNPP) liquid substrate system for ELISA, and phosphate buffered saline (PBS, product no P3744), pH 7.6 (25 °C), were purchased from Sigma-Aldrich (St. Louis, MO, USA). Goat anti-rabbit IgG antibody labeled with DyLight 549 (DL549 anti-rabbit IgG) was purchased from Jackson ImmunoResearch (West Grove, PA, USA). Mouse monoclonal anti-Pf HRP2 IgG antibodies (ABMAL-0445) and mouse monoclonal anti-Pf HRP2 IgM antibodies (ABMAL-0444) were purchased from Arista Biologicals (Allentown, PA, USA). Pf HRP2 (A3000) was purchased from CTK Biotech (San Diego, CA, USA). We conjugated the antibody against Pf HRP2 (ABMAL-0445, Arista Biologicals) with alkaline phosphatase using an EZ-Link maleimide-activated alkaline phosphatase kit (Pierce Biotechnology, Rockford, IL, USA). All chemicals and reagents were used as received without further purification.

The Craft Robo Pro electronic craft cutter (Graphtec Corporation, Tokyo, Japan) was obtained from Silhouette America Inc. (Orem, UT, USA). The 3D printer was obtained from Dimension 3D, Stratasys Inc. (Eden Prairie, MN, USA). Absorbance and fluorescence measurements were performed using a microtiter plate reader (model SpectraMax M2, Molecular Devices, Vienna, VA, USA). Fluorescence measurements were performed using a Typhoon FLA 9000 scanner (GE Healthcare, Wilmington, MA, USA). Electrochemical measurements were carried out using an electrochemical analyzer (model Autolab PGSTAT302N, Metrohm, Riverview, FL, USA).

Design and Fabrication of the Device. A “48-well plate”, comprising 48 individual devices, was fabricated from a 20 × 20 cm² sheet of chromatography paper (see Figure S1 in the Supporting Information). Paper was embossed and subsequently functionalized with decyl trichlorosilane; three electrodes were deposited adjacent to each embossed feature (Figure 1). Individual devices were cut from the sheet using scissors.

We used embossing to shape the sheet of paper into a microtiter plate using a pair of molds (one male, or projecting mold, and one female, or intaglio mold). We designed the shapes of the molds using SolidWorks (Dassault Systèmes, S. A., Vélizy, France) (see Figure S2A in the Supporting Information) and fabricated them from acrylonitrile butadiene

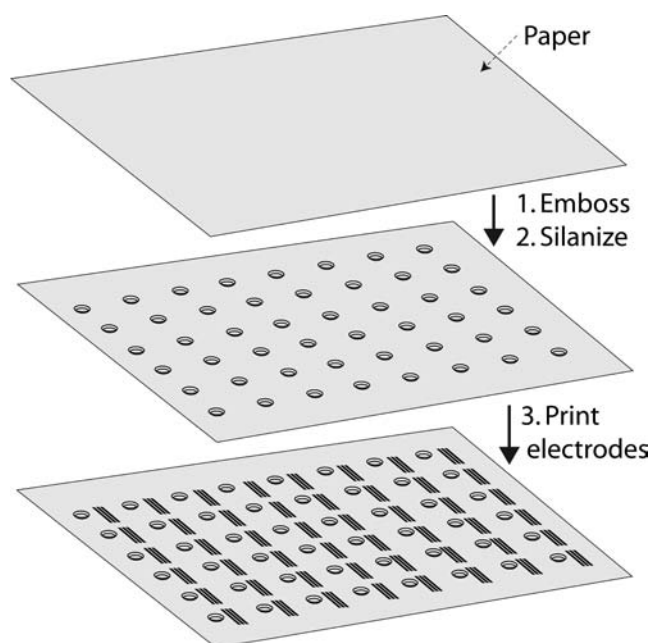


Figure 1. Fabrication of paper-based electrochemical devices. Cellulose paper is (1) embossed by 3D printed molds containing an array of circular features; (2) the embossed paper is subsequently functionalized with decyl trichlorosilane; (3) three electrodes are deposited adjacent to each embossed feature using a pen-on-paper approach (Figure S3 depicts the process).

styrene (ABS) using a 3D printer (see Figure S2B in the Supporting Information). We wet a flat sheet of chromatography paper with ethanol using a spray bottle in order to render paper easier to shape, and then we placed it between the pair of molds and pressed it manually. The embossed paper was then removed and allowed to dry in air. The fast evaporation of the ethanol helped to prevent undesired warping of the paper.

We functionalized chromatography paper using a silanization reaction conducted in a chamber with a volume of 0.01 m^3 at a temperature set at $105 \text{ }^\circ\text{C}$.⁵ The silanizing reagent, decyl trichlorosilane, was transferred into a glass vial and placed inside the chamber together with the samples. Each experiment typically required approximately 100 mg of silane in 5 mL of anhydrous toluene. Decyl trichlorosilane was vaporized at $95 \text{ }^\circ\text{C}$ under reduced pressure ($\sim 30 \text{ mbar}$, 0.03 atm) and allowed to react with the cellulose paper for 5 min. Diffusion and convection inside the reaction chamber was sufficient for an even distribution of the organosilane within the chamber. We refer to the paper produced according to this protocol using decyl trichlorosilane as C_{10}^{H} paper.

We printed graphite electrodes on the surface of hydrophobic paper using a pen-on-paper⁵⁰ approach. The template of the three-electrode system, comprising working (WE), counter (CE), and pseudoreference (RE) electrodes, was designed using Adobe Illustrator (Adobe Systems Inc., San Jose, CA). All three electrodes were printed using graphite ink in order to minimize cost and simplify the procedure.

We used a $960\text{-}\mu\text{m}$ rollerball pen (Gelly Roll Metallic pen, Sakura, Inc., Japan) to dispense the graphite ink. To clean the pen, the ink barrel was separated from the rollerball tip, and the commercial ink was removed using compressed air followed by flushing with ethanol and sonicating in a bath of distilled water. Graphite ink was loaded into the pen, and the ink was initially forced through the rollerball tip by applying a pulse of

compressed air to the back of the ink barrel. The pen was installed in the blade-set of the Craft Robo Pro electronic craft cutter, and the electrodes were printed according to the digital file. Figure S3 in the Supporting Information depicts the process. Printed graphite features were allowed to dry at room temperature ($23 \pm 2 \text{ }^\circ\text{C}$) or a minimum of 1 h before being used in experiments. Each printed feature has an area of $\sim 0.8 \times 16 \text{ mm}^2$, of which $0.8 \times 5 \text{ mm}^2$ ($0.040 \pm 0.002 \text{ cm}^2$) serves as active electrode (WE, CE, or RE), in contact with the aqueous solution, and $\sim 0.8 \times 11 \text{ mm}^2$ ($0.088 \pm 0.005 \text{ cm}^2$) serves as a connection and is inserted into a holder (see Figure S4 in the Supporting Information) to connect with the potentiostat.

Evaluation of the Immobilization of Proteins on the Surface of Microwells Embossed in Hydrophobic R^{H} Paper. All experiments were carried out at room temperature ($23 \pm 2 \text{ }^\circ\text{C}$). First, we tested the ability of C_{10}^{H} paper to adsorb proteins (antigens and antibodies) onto its surface by evaluating the immobilization of a fluorescently labeled antibody: goat anti-rabbit IgG labeled with DyLight 549 (DL549 anti-rabbit IgG). We prepared microtiter plates with microwells embossed in chromatography paper functionalized with decyl trichlorosilane. We incubated a solution of fluorescent antibody (10 and $25 \mu\text{g mL}^{-1}$ DL549 anti-rabbit IgG in PBS, pH 7.6) or blank (PBS, pH 7.6) in the microwells ($n = 7$) for 10 min. Following the incubation, the solution was removed, and the microwells ($n = 7$) were washed three times with $100 \mu\text{L}$ of PBST (PBS, 0.05% Tween-20, pH 7.6). We then recorded the fluorescence intensity of the wells using a fluorescence scanner, with excitation and emission wavelengths of 544 and 590 nm, respectively. The difference in fluorescence intensity between the blank and the samples incubated with DL549 anti-rabbit IgG (10 and $25 \mu\text{g mL}^{-1}$), followed by washing, would indicate that the antibody was immobilized on the surface of the well and did not elute with the washing buffer.

We then tested the ability of a solution of a standard blocking solution (1% BSA in PBS, pH 7.6) to prevent the nonspecific adsorption of proteins on C_{10}^{H} paper. Wells were blocked by incubation for 10 min with the blocking solution. Solutions of fluorescent antibody (DL549 anti-rabbit IgG at 10 and $25 \mu\text{g mL}^{-1}$ in PBS, pH 7.6) and blank solutions (PBS, pH 7.6) were incubated in either blocked or unblocked wells for 10 min. The wells were washed with $100 \mu\text{L}$ of PBST three times, and the fluorescence intensity of the wells was recorded using a fluorescence scanner, with excitation and emission wavelengths of 544 and 590 nm, respectively. If the BSA solution works effectively as a blocking agent, then it should prevent the adsorption of antibodies to paper. The unbound antibodies would elute in the washing buffer, and, consequently, the blocked wells should have fluorescence intensities undistinguishable from that of the background.

The mean fluorescence intensities of any two samples were compared using an unpaired Student's *t* test (GraphPad Software, San Diego, CA, USA; www.graphpad.com). We assumed statistical significance if $P < 0.05$.

Electrochemical Analysis. We performed cyclic voltammetry (CV) and square-wave voltammetry (SWV) with our electrochemical device using a commercial potentiostat (Autolab PGSTAT12, Metrohm). All electrochemical measurements were carried out at room temperature ($23 \pm 2 \text{ }^\circ\text{C}$). We connected the paper device to the potentiostat using a reusable magnetic PDMS holder (Figure S4). The PDMS holder consisted of two parts (a top part, $3 \times 1.1 \times 0.5 \text{ cm}^3$, and a

bottom part, $3 \times 6 \times 0.5 \text{ cm}^3$), each cast in PDMS and containing an embedded magnet (Neodymium Magnets $1/2 \times 1/4 \times 1/4 \text{ in.}^3$ Bar N48, Apex Magnets, Petersburg, WV, USA). The top part of the holder contained a 3-pin, 2.54 mm pitch header that connected the electrodes to the potentiostat. The paper device was placed between the two parts of the holder, with the electrodes in contact with the pin header. The two embedded magnets allowed the two parts of the holder to self-align and the holder to open and close easily. This holder can also be used to interface with portable electrochemical readers such as the one developed by Nemiroski et al.²

To evaluate the performance of the printed electrodes, we used cyclic voltammetry (CV). We performed this analysis using ferrocenecarboxylic acid (FCA) at six different concentrations (10, 50, 100, 250, 500, and $1000 \mu\text{mol L}^{-1}$ in PBS, pH 7.6) and 4-amino phenol (pAP) at three different concentrations (10, 100, $1000 \mu\text{mol L}^{-1}$ in PBS, pH 7.6), at a scan rate of 100 mV s^{-1} . The electrochemical behavior of the electrodes was further characterized by cyclic voltammetry using a solution of FCA ($100 \mu\text{mol L}^{-1}$ in PBS, pH 7.6) at different scan rates (10, 50, 100, 200, and 300 mV s^{-1}).

Cyclic voltammetry is not an ideal method for accurate quantitation of electroactive species because the correction for the capacitive current is typically uncertain.⁵¹ In order to increase the sensitivity of our measurements, we used square-wave voltammetry (SWV), a fast electrochemical technique developed by Osteryoung and O'Dea.⁵² The electrochemical signal of the pAP produced in the enzymatic amplification step of the ELISA was recorded using SWV (scan potential between -0.3 and 0.3 V ; pulse amplitude = 0.10 V ; square-wave frequency = 10 Hz ; step height = 0.005 V).

Electrochemical Direct ELISA for Detection of Rabbit IgG. All experiments were carried out at room temperature ($23 \pm 2 \text{ }^\circ\text{C}$). Initially, each well was washed three times with $100 \mu\text{L}$ volumes of a solution of PBST. A drop ($10 \mu\text{L}$) of a solution with a known concentration of rabbit IgG, in 10-fold serial dilutions between 25 pg mL^{-1} ($0.167 \text{ pmol L}^{-1}$) and $25 \mu\text{g mL}^{-1}$ (167 nmol L^{-1}), was added to each embossed well, and the wells were covered with a removable adhesive plastic (PET/EVA/LDPE, Fellowes sheet) and allowed to incubate for 30 min. The solution was then aspirated from the wells with a pipet, and the surface of the wells was rinsed with $50 \mu\text{L}$ of PBS (pH 7.6). Next, the surface was blocked with $50 \mu\text{L}$ of a 1% solution of BSA in PBST for 5 min. The solution was removed, and the well was washed with $50 \mu\text{L}$ of PBST. A volume of $50 \mu\text{L}$ of anti-rabbit IgG ALP was added and incubated for 5 min. The plate was washed three times with PBST. The enzymatic amplification was performed by adding $50 \mu\text{L}$ of 5 mmol L^{-1} pAPP in a buffer solution ($1 \times$ PBS buffer supplemented with $10 \text{ mmol L}^{-1} \text{ MgCl}_2$, pH 9.5). After the enzymatic reaction was allowed to occur for 10 min, the device was folded, and the electrodes were allowed to come into contact with the solution. The electrochemical signal of the pAP produced was recorded using square-wave voltammetry (SWV) (scan potential between -0.3 and 0.3 V ; pulse amplitude = 0.10 V ; square-wave frequency = 10 Hz ; step height = 0.005 V). The LOD was defined by the concentration that resulted in a signal equal to the average signal of the control, i.e., at zero concentration of IgG, plus three times the standard deviation of the signal of the control.

Electrochemical Sandwich ELISA for Detection of Pf HRP2. All experiments were carried out at room temperature ($23 \pm 2 \text{ }^\circ\text{C}$). Each well was washed three times with $100 \mu\text{L}$ of

a solution of PBST. The wells were coated by incubation of $50 \mu\text{L}$ of capture antibody (anti-Pf HRP2 IgM) at a concentration of $10 \mu\text{g mL}^{-1}$ in PBST for 1 h. The wells were washed three times with PBST and then blocked using $50 \mu\text{L}$ of a 1% solution of BSA in PBST for 10 min. The solutions of recombinant Pf HRP2 were prepared in a 10% m/m solution of human serum in PBST. The wells were incubated with $50 \mu\text{L}$ per well of solutions of human serum spiked with known concentrations of Pf HRP2 for 30 min. The wells were then washed three times with $50 \mu\text{L}$ PBST and incubated with $50 \mu\text{L}$ of ALP-conjugated detection antibody ($1 \mu\text{g mL}^{-1}$ in PBS, pH 7.6, anti-Pf HRP2 IgG-ALP). After incubation for 20 min under agitation, the solution was aspirated. The wells were washed five times with $50 \mu\text{L}$ of PBST instead of three times because we found that it gave lower background for this assay. Detection was completed by adding $50 \mu\text{L}$ of 5 mmol L^{-1} pAPP in a buffer ($1 \times$ PBS buffer supplemented with $10 \text{ mmol L}^{-1} \text{ MgCl}_2$, pH 9.5) at room temperature in each well. After the enzymatic reaction was allowed to occur for 15 min, the device was folded, the electrodes were allowed to come into contact with the solution, and the signal was read using SWV (scan potential between -0.3 and 0.3 V ; pulse amplitude = 0.10 V ; square-wave frequency = 10 Hz ; step height = 0.005 V). The LOD was defined by the concentration that results in a signal that was equal to the average signal of the control, i.e., at zero concentration of Pf HRP2, plus three times the standard deviation in the signal of the control.

Colorimetric Direct ELISA for Detection of Rabbit IgG.

A volume ($200 \mu\text{L}$) of a solution of antigen (rabbit IgG in $1 \times$ PBS, pH 7.6), in 10-fold serial dilutions between 25 pg mL^{-1} ($0.167 \text{ pmol L}^{-1}$) and $25 \mu\text{g mL}^{-1}$ (167 nmol L^{-1}), was added to wells in a 96-well polystyrene plate and incubated for 16 h at $4 \text{ }^\circ\text{C}$. The solution was removed from the wells, and the wells were washed with $200 \mu\text{L}$ of PBS (pH 7.6). Next, the surface of the well was blocked with $200 \mu\text{L}$ of a 1% solution of BSA in PBST for 1 h at room temperature ($23 \pm 2 \text{ }^\circ\text{C}$). The solution was removed, and the well was washed with $200 \mu\text{L}$ of PBST. A volume of $200 \mu\text{L}$ of anti-rabbit IgG-ALP was added and incubated for 1 h at room temperature ($23 \pm 2 \text{ }^\circ\text{C}$). The plate was washed three times with PBST. The enzymatic amplification was performed by adding $200 \mu\text{L}$ of alkaline phosphatase yellow (pNPP) liquid substrate system for ELISA, and the reaction was allowed to proceed for 20 min at room temperature ($23 \pm 2 \text{ }^\circ\text{C}$). Absorbance was recorded at 405 nm using a microtiter plate reader.

Colorimetric Sandwich ELISA for Detection of Pf HRP2. The wells of a 96-well polystyrene plate were coated by incubation of $200 \mu\text{L}$ of capture antibody (anti-Pf HRP2 IgM) at a concentration of $10 \mu\text{g mL}^{-1}$ in PBST for 16 h at $4 \text{ }^\circ\text{C}$. The wells were washed with $200 \mu\text{L}$ PBST and then blocked using $200 \mu\text{L}$ of a 1% solution of BSA in PBST for 1 h at room temperature. The solutions of recombinant Pf HRP2 were prepared in a 10 wt % solution of human serum in PBST. The wells were incubated with $200 \mu\text{L}$ per well of solutions of human serum spiked with known concentrations of Pf HRP2 for 1 h at room temperature. The wells were then washed three times with $200 \mu\text{L}$ PBST and incubated with $200 \mu\text{L}$ of ALP-conjugated detection antibody ($1 \mu\text{g mL}^{-1}$ in PBS, pH 7.6, anti-Pf HRP2 IgG-ALP). After incubation for 1 h at room temperature under agitation, the solution was removed, and the plate was washed three times with PBST. Detection was completed by adding $200 \mu\text{L}$ of alkaline phosphatase yellow (pNPP) liquid substrate system for ELISA, and the reaction

was allowed to proceed for 20 min at room temperature (23 ± 2 °C). Absorbance was recorded at 405 nm using a microtiter plate reader.

RESULTS AND DISCUSSION

Design and Fabrication of the Device. We have chosen paper as a substrate for the fabrication of the electroanalytical device because it is widely available, inexpensive, lightweight, flexible, easily creased, easily printed with conductive materials, and embossed or folded into 3D configurations; it also does not break into sharps and can be disposed of easily by burning. The ease of modifying its surface chemistry allowed us to render the paper hydrophobic using a 5 min vapor-phase treatment with decyl trichlorosilane ($C_{10}H$).⁵ The modified paper can be easily printed with conductive inks,⁴⁵ and it facilitates the physical adsorption of biomolecules on its surface through hydrophobic interactions. The roughness of the paper affords a large surface area for the adsorption of proteins on the surface of the functionalized paper. We took advantage of these properties to immobilize antigens and antibodies on the surface of wells in hydrophobic paper. Embossing was chosen to shape the paper into a microtiter microplate because it is simple, rapid, and requires inexpensive equipment (i.e., reusable molds generated using a 3D printer). Embossing is also compatible with mass fabrication methods such as reel-to-reel manufacture processes.

We produced linear arrays of electrodes (a graphite working electrode, a graphite counter electrode, and a graphite quasi-reference electrode) spaced 1.5 mm apart using a 960- μm rollerball pen filled with colloidal graphite ink on $C_{10}H$ paper (Figure 1). The rollerball pen filled with conductive graphite ink, under the control of a craft plotter, can transfer an easily modifiable digital pattern onto a sheet of paper to generate printed electrodes within minutes. This printing technique is useful for rapid prototyping and mass customization of electronic devices because it does not require custom-patterned components, such as screens, stencils, and masks. This pen-on-paper approach was first introduced by Russo et al.⁵⁰ and was further developed by Mirica et al.⁵³ to draw gas sensors on paper. In conjunction with the craft plotter, this approach afforded us a high degree of reproducibility in the printing of the electrodes, a high degree of flexibility in modifying and optimizing the design of the electrodes, and a fast method of fabricating relatively large numbers of electrodes (~ 10 min to print a file comprising 70 three-electrode cells) (see Figure S3 in the Supporting Information).

To minimize the fouling of the electrode by compounds required for a typical ELISA, we have spatially separated the process involved in the capture of the antigen and the detection of the electroactive enzymatic product. The electroanalytical device incorporates printed electrodes proximal to, but not in contact with, the embossed microwell on the surface where the immobilization of the antigen and the subsequent recognition events occur. The flexibility and foldability of the paper substrates allows us to bring the electrodes into contact with the reaction mixture only when the electrochemical detection step was ready to be performed. After completing the addition and removal of the series of reagents required for the ELISA, the device was folded along a central crease to bring the electrodes in contact with the solution of the electroactive product of the enzymatic reaction (Figure 2).

Evaluation of the Immobilization of Proteins on the Surface of Microwells Embossed in Hydrophobic R^H Paper. We used a fluorescently labeled antibody, DL549

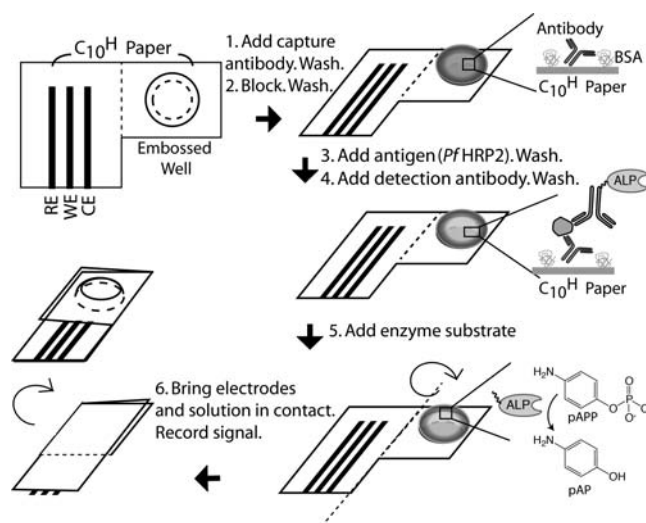


Figure 2. Schematic illustration of the approach of electrochemical immunoassay in hydrophobic paper microwells. The electrochemical sandwich ELISA depicted here comprises six steps: (1) immobilizing capture antibodies (2) blocking with a solution of BSA, (3) binding of antigen to antibody, (4) binding of detection antibody, conjugated to ALP, to antigen, (5) ALP-mediated conversion of an electrochemically inactive substrate (pAPP) into electrochemically active pAP, and (6) electrochemical measurement.

anti-rabbit IgG, to test the ability of the $C_{10}H$ paper to adsorb antibodies and protein antigens on the surface as well as to evaluate the ability of bovine serum albumin (BSA) to block remaining active sites. Using Student's *t* test, we compared the mean values of fluorescence intensity in wells incubated with solutions of the fluorescently labeled antibody, followed by triple wash with PBST, with the fluorescence intensity of the blank (Figure S5). The increase in fluorescence intensity in the unblocked wells compared to the blank was significant (95% confidence interval; $P < 0.0001$ for both 10 and 25 $\text{ng } \mu\text{L}^{-1}$ of antibody), confirming the adsorption of the fluorescent antibody on the surface of the hydrophobic $C_{10}H$ paper. The extent of the immobilization increased with increased concentration of antibody in the solution (the mean values for the fluorescence intensity following incubation with 10 and 25 $\text{ng } \mu\text{L}^{-1}$ of antibody, followed by triple wash with PBST, are different at a 95% confidence level; $P = 0.0207$), suggesting that concentrations of antibody under 25 $\text{ng } \mu\text{L}^{-1}$ are below the saturation point of the well.

To test the ability of a protein solution to block the surface of the wells within $C_{10}H$ paper, we incubated the wells with solutions of BSA (1% in PBST) for 10 min. Solutions of DL549 anti-rabbit IgG were then added to wells that were blocked or unblocked, incubated for 10 min, and then washed with PBST. In the wells that were blocked, the fluorescent signal was not significantly different from the background (95% confidence interval; $P = 0.1199$ for 25 $\text{ng } \mu\text{L}^{-1}$ of antibody), whereas the wells that were unblocked produced higher fluorescent signals. Thus, the results showed that a solution of BSA can be used to block nonspecific adsorption of proteins on the surface of $C_{10}H$ hydrophobic paper and a solution of PBST can be used effectively to remove unbound proteins from blocked wells.

Recording the Analytical Signal. To evaluate the performance of the electrodes over a potential window, we recorded the cyclic voltammograms (CVs) of ferrocene carboxylic acid (FCA) at six different concentrations (10, 50,

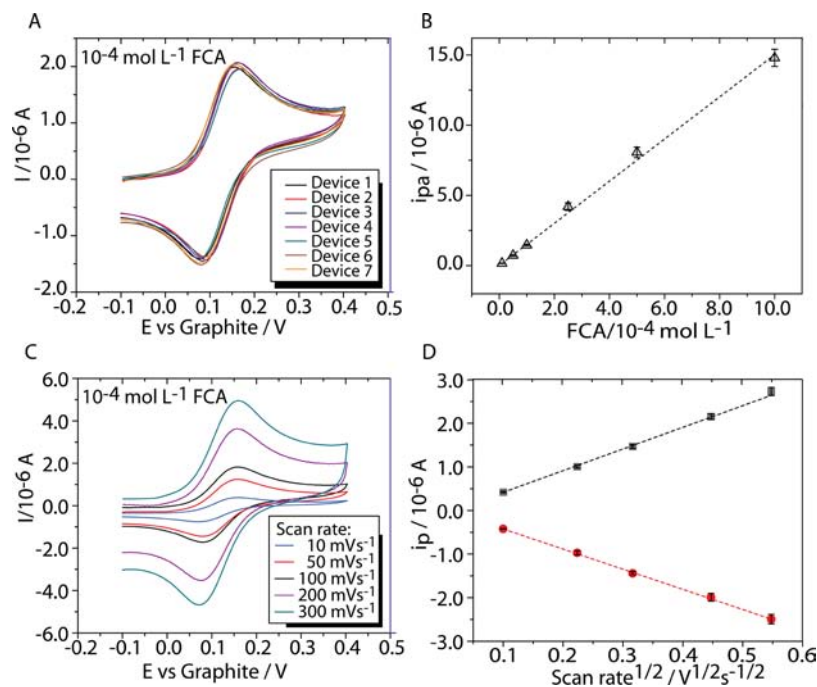


Figure 3. (A) Cyclic voltammograms of a solution of FCA ($100 \mu\text{mol L}^{-1}$ in PBS, pH 7.6) for seven independently fabricated devices. (B) Plot of relation between concentration of FCA in PBS, pH 7.6, and anodic peak current (i_{pa}), measured at 100 mV s^{-1} . The relationship is linear, with $R^2 = 0.997$. (C) Cyclic voltammograms of a solution of FCA ($100 \mu\text{mol L}^{-1}$ in PBS, pH 7.6) at different scan rates (10, 50, 100, 200, 300 mV s^{-1}). (D) Anodic (black) and cathodic (red) peak currents as a function of square root of the scan rate. In panels B and D, each datum represents the average of seven independent measurements, and the error bars represent the standard deviation from the average.

100, 250, 500, and $1000 \mu\text{mol L}^{-1}$ in PBS pH 7.6). FCA is a redox probe with well-characterized electrochemical behavior. Figure 3A shows the variation in the CVs of a solution of FCA ($100 \mu\text{mol L}^{-1}$ in PBS, pH 7.6) recorded using seven different devices. We observed very small device-to-device variation in the performance of the electrodes, as indicated by the small relative standard deviation (RSD, defined as the percentage ratio of the standard deviation to the mean of the distribution) of 2.9% in the peak current, i_p (Figure 3A). The peak current potential separation $\Delta E_p = E_{pa} - E_{pc}$ has an average value of $63 \pm 6 \text{ mV}$; this value indicates the presence of an almost reversible process with a fast electron transfer ($i_{pc}/i_{pa} = 1.02 \pm 0.03$).

To characterize the variation in the performance of the electrodes between different batches as a function of the concentration of the analyte, we determined the anodic peak current, i_{pa} , measured from the decaying cathodic current as a baseline.⁵¹ Figure 3B shows that the anodic peak current is linearly proportional to the concentration of FCA ($R^2 = 0.997$).

To test whether the electrochemical process is adsorption- or diffusion-controlled, we characterized the behavior of the electrodes as a function of scan rate. We recorded cyclic voltammograms of $100 \mu\text{mol L}^{-1}$ FCA in PBS, pH 7.6, at scan rates between 10 and 300 mV s^{-1} , and observed that the anodic and cathodic peak currents (i_{pa} and i_{pc}) are linearly proportional to the square root of the scan rate ($R^2 = 0.998$ and 0.999 , respectively) (Figure 3D). This result indicates that the process is diffusion-controlled. There is no significant variation of ΔE_p with the scan rate or with concentration (see Figure S7 in the Supporting Information), suggesting that there is no significant uncompensated solution resistance and that the kinetics of the electron transfer process in the system is fast. The behavior is similar to the behavior observed in traditional electrochemical

cells, suggesting that the rate of the electrochemical reaction is governed by the diffusion of FCA into the surface of the planar electrode.

After characterizing the reproducibility of the fabrication method and the electrochemical behavior of the device using a well-known redox probe, FCA, we analyzed the response of the system to an electroactive species that can be used to quantify the signal in an electrochemical ELISA. There are several examples of enzyme/substrate pairs that can be used to generate electroactive products. We have chosen alkaline phosphatase (ALP) as the enzyme and 4-aminophenyl phosphate (pAPP) as the substrate because a wide variety of ALP-conjugated antibodies are commercially available and because ALP and pAPP generate an electrochemically active product, pAP, that can be oxidized to a quinone imine⁵⁴ at a relatively low potential ($\sim 200 \text{ mV}$ vs graphite quasi-reference electrode). As the noise in electrochemical detection typically increases with increasing potential, this low oxidation potential of pAP is advantageous. This low potential also makes the interference from the oxidation of other species in the sample unlikely. We have characterized the behavior of the electrodes with pAP using CV and observed that the anodic peak current varies linearly with the concentration of pAP ($R^2 = 0.993$) (see Figure S6 in the Supporting Information). The variation of the peak current potential separation with concentration of pAP is shown in Figure S8. At high concentrations ($>100 \mu\text{mol L}^{-1}$), pAP shows quasi-reversible behavior, with a peak current potential separation of $130 \pm 17 \text{ mV}$ at 1 mmol L^{-1} concentration in PBS (see Figure S7 and the discussion in section S3 of the Supporting Information).

Electrochemical Direct ELISA for Detection of Rabbit IgG. We used rabbit IgG as a model antigen⁴⁸ and anti-rabbit IgG-ALP conjugate as the detection antibody to test the

performance of our device in a direct ELISA. Rabbit IgG ($10 \mu\text{L}$) was applied to each well in 10-fold dilutions ranging from $0.167 \text{ pmol L}^{-1}$ to 167 nmol L^{-1} , the wells were covered, and the solution was allowed to incubate for 30 min at room temperature. After washing with PBST and blocking the surface of the well with a solution of BSA, the anti-rabbit IgG–ALP conjugate was added to each well and incubated for 10 min at room temperature to allow binding with the rabbit IgG. After the excess was washed away, a solution of the electrochemical substrate pAPP was added to the microwells. The conversion of pAPP to electrochemically active pAP was allowed to proceed for 10 min before the device was folded along the central crease to bring the electrodes into contact with the solution of the electroactive enzymatic product, and the electrochemical signal was measured using SWV (Figure 4).

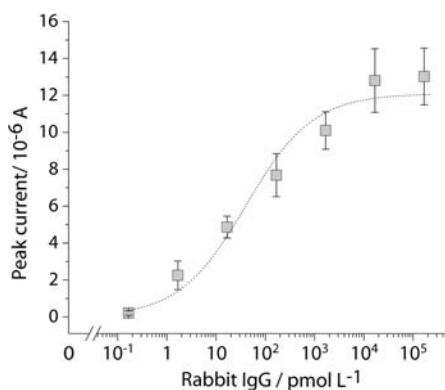


Figure 4. Effect of concentration of IgG on the SWV peak current in a direct ELISA. The average value of the blank was subtracted from each measurement. Each datum is the mean of seven replicates, and the error bars are standard deviations of the measurements. The limit of detection is estimated to be 2 pmol L^{-1} . The R^2 value of the curve fit to the data using the Hill equation is 0.978. The curve is approximately linear between the concentrations of 10 and 1000 pmol L^{-1} of rabbit IgG per well ($R^2 = 0.998$).

The parameters for SWV measurement were identified in preliminary trials to provide the highest signal-to-noise ratio in the detection of a 100 nmol L^{-1} solution of pAP in PBS (data not shown); these parameters were chosen as a pulse amplitude of 0.10 V , a square-wave frequency of 10 Hz , and a step height of 0.005 V for scanning the potential between -0.3 and 0.3 V vs graphite quasi-reference electrode. The measurements were performed using a commercial potentiostat; the parameters are fully compatible with the portable electrochemical reader developed by Nemiroski et al.²

We generated a calibration curve of the peak current recorded by SWV versus the concentration of rabbit IgG at concentrations ranging from $0.167 \text{ pmol L}^{-1}$ to 167 nmol L^{-1} (in PBS, pH 7.6), as shown in Figure 4. The peak current of pAP was found to be proportional to the concentration of rabbit IgG. We can approximate this curve as linear in the concentration range of 10 – 1000 pmol L^{-1} using a simple linear regression ($R^2 = 0.998$).

At the present state of development, the LOD of our electrochemical direct ELISA for rabbit IgG is 2 pmol L^{-1} (0.3 ng mL^{-1}). This LOD was lower than the one we determined for conventional absorbance ELISA (8 ng mL^{-1}) using the same antigen/antibody pair. The detection limit reached using our device is comparable with values reported in previously published studies describing electrochemical ELISA carried out

with different devices and antigen/antibody pairs. For example, Nemiroski et al.² reported a LOD of 20 ng mL^{-1} for *Pf* HRP2, Bhimji et al.⁸ reported a LOD of 1 ng mL^{-1} for HIV-1 antibodies, Sun et al.⁵⁵ reported a LOD of 0.5 ng mL^{-1} for cucumber mosaic virus, Liu et al.⁴ reported a LOD of 0.02 ng mL^{-1} for α -fetoprotein, and Sha et al.³ reported a LOD of 0.5 pg mL^{-1} for the detection of dentine sialophosphoprotein.

Electrochemical Sandwich ELISA for Detection of *Pf* HRP2. We used our device to detect and quantify levels of *Pf* HRP2 spiked into diluted human serum using a sandwich ELISA assay. We immobilized the capture antibodies (mouse anti-*Pf* HRP2 IgM) on the hydrophobic C_{10}^{H} paper surface by passive adsorption. We conjugated the detection antibody (mouse anti-*Pf* HRP2 IgG) to ALP in order to minimize the number of incubation and washing steps in the assay.

We used human serum samples spiked with recombinant *Pf* HRP2 at concentrations ranging from 1 to 10^6 ng mL^{-1} as our test samples and subsequently generated a calibration curve for the concentration of *Pf* HRP2 protein vs the peak current of pAP, as recorded by SWV (Figure 5). The LOD for our device was 4 ng mL^{-1} (102 pmol L^{-1}). The LOD we measured in a conventional colorimetric ELISA was 18 ng mL^{-1} for the same antigen and antibody pair.

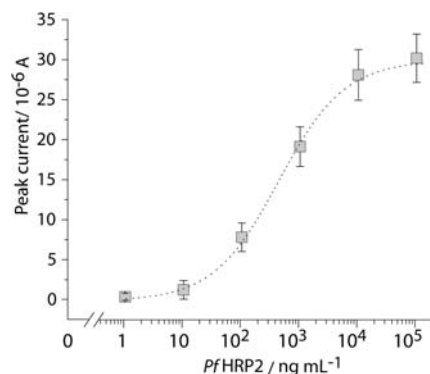


Figure 5. Effect of concentration of *Pf* HRP2 on the SWV peak current in a sandwich ELISA. The average value of the blank was subtracted from each measurement. Each datum is the mean of seven replicates, and the error bars are standard deviations of the measurements. The limit of detection is estimated to be 4 ng mL^{-1} . The R^2 value of the curve fit to the data using the Hill equation is 0.988. We can approximate the curve as linear between the concentrations of 10 and 1000 ng mL^{-1} of *Pf* HRP2 per well ($R^2 = 0.989$).

According to a study by Dondorp et al., the mean (95% CI) concentration of *Pf* HRP2 in the plasma of 337 patients with falciparum malaria was $0.84 \mu\text{g mL}^{-1}$, corresponding to a range of 0.57 – $1.11 \mu\text{g mL}^{-1}$.⁵⁶ This result suggests that our assay can easily and accurately detect the presence of *Pf* HRP2 in concentrations that are clinically relevant.

CONCLUSIONS

This study describes the development of a device for an electrochemical ELISA designed, ultimately, for integration into systems for low-resource settings. Made entirely from hydrophobic paper and printed carbon electrodes, our device is versatile: it can be used for direct, indirect, or sandwich ELISA and can be readily adapted to detect other analytes for which appropriate antibodies and antigens have been developed.

Arrays of such devices can interface with multichannel electrochemical readers to perform multiplex analyses.

This device has five significant features: (i) it is quantitative and sensitive, (ii) it is cost-effective (~\$0.005 per device for materials, not including the cost of the biochemical reagents), due to the inexpensive materials and method used for its fabrication, (iii) it is easily stored and transported, (iv) contaminated devices can be easily disposed of after use (by incineration), and (v) the equipment used for electrochemical detection is lighter, smaller, and less expensive than conventional spectrophotometers or optical scanners. The paper-based device described here can be coupled with miniaturized electrochemical readers with performance comparable to that of commercial potentiostats, as described previously by Nemiroski et al.² The cost of these devices along with the ease of interfacing with telephone and web-based systems for transferring information to medical and public health personnel, and for processing and storage, has the potential to broaden the applicability of electrochemical analysis in field settings.

At its present demonstration level of development, this work does not, of course, meet all of the demands of low-resource settings. The need to add and remove small fixed volumes of reagents manually and sequentially still limits the practicality of this device in field applications. To simplify the user interface, the integration with other technologies for reagent storage and fluid delivery remains to be explored. Having recently demonstrated the development of open-channel microfluidic systems in omniphobic and hydrophobic paper,^{57,58} of particular importance for future integration with our device are two technologies: “mChip”,^{59,60} a method to introduce metered plugs of reagents, separated by air spacers, into microfluidic channels, and “blister pumps”,^{61,62} a method that uses on chip “blisters” that can be manually actuated by the user to transport fluids through microfluidic channels on the device. While future development is still needed to render these devices fieldable, the work demonstrates the potential of this kind of device and analysis.

■ ASSOCIATED CONTENT

■ Supporting Information

Image depicting a 48-well plate comprising 48 individual electrochemical cells embossed in hydrophobic R^H paper; schematic diagram showing the design and dimensions of the molds used for embossing; representation of the technique used for the printing of electrodes; image depicting the PDMS holder used to connect the paper-based device to a potentiostat; analysis of the immobilization of a fluorescent antibody on the surface of R^H paper; analysis of the electrochemical behavior of a set of independently fabricated devices in response to pAP; analysis of the variation of the peak current potential separation with scan rate and with concentration of analyte; discussion of the cost of fabrication per device; and discussion of the environmental impact of disposing of devices by incineration. This material is available free of charge via the Internet at <http://pubs.acs.org>.

■ AUTHOR INFORMATION

Corresponding Authors

*(M.T.F.-A.) E-mail: mtfernandeza@uniovi.es.

*(G.M.W.) E-mail: gwhitesides@gmwhgroup.harvard.edu.

Notes

The authors declare no competing financial interest.

■ ACKNOWLEDGMENTS

This work was funded in part by the Bill & Melinda Gates Foundation under award 51308. M.T. Fernández-Abedul thanks the University of Oviedo (Campus de Excelencia Internacional) and the Spanish Ministry of Economy and Competitiveness (project MICINN CTQ2011-25814) for funding her stay at Harvard University. We thank Jeremy Schonhorn, Jason Rolland, and Christina Swanson from Diagnostics for All (Cambridge, MA) and Maria-Nefeli Tsaloglou from Harvard University, for helpful discussions.

■ REFERENCES

- (1) Maxwell, E. J.; Mazzeo, A. D.; Whitesides, G. M. *MRS Bull.* **2013**, *38*, 309–314.
- (2) Nemiroski, A.; Christodouleas, D.; Hennek, J.; Maxwell, E. J.; Fernández-Abedul, M. T.; Whitesides, G. M. *Proc. Natl. Acad. Sci. U.S.A.* **2014**, *111*, 11984–11989.
- (3) Sha, H.; Bai, Y.; Li, S.; Wang, X.; Yin, Y. *Am. J. Orthod. Dentofacial Orthop.* **2014**, *145*, 36–40.
- (4) Liu, Q. L.; Yan, X. H.; Yin, X. M.; Situ, B.; Zhou, H. K.; Lin, L.; Li, B.; Gan, N.; Zheng, L. *Molecules* **2013**, *18*, 12675–12686.
- (5) Glavan, A. C.; Martinez, R. V.; Subramaniam, A. B.; Yoon, H. J.; Nunes, R. M. D.; Lange, H.; Thuo, M. M.; Whitesides, G. M. *Adv. Funct. Mater.* **2014**, *24*, 60–70.
- (6) Dequaire, M.; Degrand, C.; Limoges, B. *Anal. Chem.* **2000**, *72*, 5521–5528.
- (7) Aguilar, Z. P.; Vandaveer, W. R.; Fritsch, I. *Anal. Chem.* **2002**, *74*, 3321–3329.
- (8) Bhimji, A.; Zaragoza, A. A.; Live, L. S.; Kelley, S. O. *Anal. Chem.* **2013**, *85*, 6813–6819.
- (9) Pampalakis, G.; Kelley, S. O. *Analyst* **2009**, *134*, 447–449.
- (10) Rossier, J. S.; Girault, H. H. *Lab Chip* **2001**, *1*, 153–157.
- (11) Tang, D. P.; Su, B. L.; Tang, J.; Ren, J. J.; Chen, G. N. *Anal. Chem.* **2010**, *82*, 1527–1534.
- (12) Bange, A.; Halsall, H. B.; Heineman, W. R. *Biosens. Bioelectron.* **2005**, *20*, 2488–2503.
- (13) Gonzalez-Garcia, M. B.; Fernandez-Sanchez, C.; Costa-Garcia, A. *Biosens. Bioelectron.* **2000**, *15*, 315–321.
- (14) Niwa, O.; Xu, Y.; Halsall, H. B.; Heineman, W. R. *Anal. Chem.* **1993**, *65*, 1559–1563.
- (15) Fernandez-Sanchez, C.; Gonzalez-Garcia, M. B.; Costa-Garcia, A. *Biosens. Bioelectron.* **2000**, *14*, 917–924.
- (16) Malhotra, R.; Patel, V.; Vaque, J. P.; Gutkind, J. S.; Rusling, J. F. *Anal. Chem.* **2010**, *82*, 3118–3123.
- (17) Ko, H.; Lee, J.; Kim, Y.; Lee, B.; Jung, C.-H.; Choi, J.-H.; Kwon, O.-S.; Shin, K. *Adv. Mater.* **2014**, *26*, 2335–2340.
- (18) *Electroanalytical Methods: Guide to Experiments and Applications*; Scholz, F., Ed.; Springer: New York, 2002.
- (19) Zang, D.; Ge, L.; Yan, M.; Song, X.; Yu, J. *Chem. Commun.* **2012**, *48*, 4683–4685.
- (20) Abad-Villar, E. M.; Fernández-Abedul, M. T.; Costa-Garcia, A. *Biosens. Bioelectron.* **2002**, *17*, 797–802.
- (21) Wise, K. D.; Najafi, K. *Science* **1991**, *254*, 1335–1342.
- (22) Pollock, N. R.; Rolland, J. P.; Kumar, S.; Beattie, P. D.; Jain, S.; Noubary, F.; Wong, V. L.; Pohlmann, R. A.; Ryan, U. S.; Whitesides, G. M. *Sci. Transl. Med.* **2012**, *4*, 152ra129.
- (23) Martinez, A. W.; Phillips, S. T.; Butte, M. J.; Whitesides, G. M. *Angew. Chem.* **2007**, *46*, 1318–1320.
- (24) Martinez, A. W.; Phillips, S. T.; Whitesides, G. M.; Carrilho, E. *Anal. Chem.* **2010**, *82*, 3–10.
- (25) Khan, M. S.; Thouas, G.; Shen, W.; Whyte, G.; Garnier, G. *Anal. Chem.* **2010**, *82*, 4158–4164.
- (26) Yager, P.; Edwards, T.; Fu, E.; Helton, K.; Nelson, K.; Tam, M. R.; Weigl, B. H. *Nature* **2006**, *442*, 412–418.

- (27) Martinez, A. W.; Phillips, S. T.; Wiley, B. J.; Gupta, M.; Whitesides, G. M. *Lab Chip* **2008**, *8*, 2146–2150.
- (28) Carrilho, E.; Martinez, A. W.; Whitesides, G. M. *Anal. Chem.* **2009**, *81*, 7091–7095.
- (29) Li, X.; Ballerini, D. R.; Shen, W. *Biomicrofluidics* **2012**, *6*, 011301–011313.
- (30) Yeo, L. Y.; Chang, H. C.; Chan, P. P.; Friend, J. R. *Small* **2011**, *7*, 12–48.
- (31) Fu, E.; Lutz, B.; Kauffman, P.; Yager, P. *Lab Chip* **2010**, *10*, 918–920.
- (32) Dungchai, W.; Chailapakul, O.; Henry, C. S. *Anal. Chem.* **2009**, *81*, 5821–5826.
- (33) Li, X.; Tian, J. F.; Garnier, G.; Shen, W. *Colloid. Surf., B* **2010**, *76*, 564–570.
- (34) Li, X.; Tian, J.; Nguyen, T.; Shen, W. *Anal. Chem.* **2008**, *80*, 9131–9134.
- (35) Abe, K.; Suzuki, K.; Citterio, D. *Anal. Chem.* **2008**, *80*, 6928–6934.
- (36) Cheng, C. M.; Martinez, A. W.; Gong, J.; Mace, C. R.; Phillips, S. T.; Carrilho, E.; Mirica, K. A.; Whitesides, G. M. *Angew. Chem.* **2010**, *49*, 4771–4774.
- (37) Liu, H.; Crooks, R. M. *J. Am. Chem. Soc.* **2011**, *133*, 17564–17566.
- (38) Wang, S.; Ge, L.; Song, X.; Yu, J.; Ge, S.; Huang, J.; Zeng, F. *Biosens. Bioelectron.* **2012**, *31*, 212–218.
- (39) Nie, Z.; Deiss, F.; Liu, X.; Akbulut, O.; Whitesides, G. M. *Lab Chip* **2010**, *10*, 3163–3169.
- (40) Cunningham, J. C.; Brenes, N. J.; Crooks, R. M. *Anal. Chem.* **2014**, *86*, 6166–6170.
- (41) Murdock, R. C.; Shen, L.; Griffin, D. K.; Kelley-Loughnane, N.; Papautsky, I.; Hagen, J. A. *Anal. Chem.* **2013**, *85*, 11634–11642.
- (42) Nie, Z.; Nijhuis, C. A.; Gong, J.; Chen, X.; Kumachev, A.; Martinez, A. W.; Narovlyansky, M.; Whitesides, G. M. *Lab Chip* **2010**, *10*, 477–483.
- (43) Liu, H.; Xiang, Y.; Lu, Y.; Crooks, R. M. *Angew. Chem.* **2012**, *124*, 7031–7034.
- (44) Renault, C.; Anderson, M. J.; Crooks, R. M. *J. Am. Chem. Soc.* **2014**, *136*, 4616–4623.
- (45) Lessing, J.; Glavan, A. C.; Walker, S. B.; Keplinger, C.; Lewis, J. A.; Whitesides, G. M. *Adv. Mater.* **2014**, *26*, 4677–4682.
- (46) Liu, H.; Li, X.; Crooks, R. M. *Anal. Chem.* **2013**, *85*, 4263–4267.
- (47) Scida, K.; Li, B. L.; Ellington, A. D.; Crooks, R. M. *Anal. Chem.* **2013**, *85*, 9713–9720.
- (48) Kissinger, P.; Heineman, W. R. *Laboratory Techniques in Electroanalytical Chemistry*, 2nd ed.; Marcel Dekker, Inc.: New York, 1996.
- (49) Wang, J. *Analytical Electrochemistry*; John Wiley & Sons: Hoboken, NJ, 2006.
- (50) Russo, A.; Ahn, B. Y.; Adams, J. J.; Duoss, E. B.; Bernhard, J. T.; Lewis, J. A. *Adv. Mater.* **2011**, *23*, 3426–3430.
- (51) Bard, A. J.; Faulkner, L. R. *Electrochemical Methods*, 2nd ed.; John Wiley & Sons: New York, 2001.
- (52) Osteryoung, J.; O'Dea, J. J. *Electroanal. Chem.* **1986**, *14*, 209–308.
- (53) Mirica, K. A.; Weis, J. G.; Schnorr, J. M.; Esser, B.; Swager, T. M. *Angew. Chem., Int. Ed.* **2012**, *51*, 10740–10745.
- (54) Tang, H. T.; Lunte, C. E.; Halsall, H. B.; Heineman, W. R. *Anal. Chim. Acta* **1988**, *214*, 187–195.
- (55) Sun, W.; Jiao, K.; Zhang, S. *Talanta* **2001**, *55*, 1211–1218.
- (56) Dondorp, A. M.; Desakorn, V.; Pongtavornpinyo, W.; Sahassananda, D.; Silamut, K.; Chotivanich, K.; Newton, P. N.; Pitisuttithum, P.; Smithyman, A. M.; White, N. J.; Day, N. P. J. *PLoS Med.* **2005**, *2*, 1047–1047.
- (57) Glavan, A. C.; Martinez, R. V.; Maxwell, E. J.; Subramaniam, A. B.; Nunes, R. M. D.; Soh, S.; Whitesides, G. M. *Lab Chip* **2013**, *13*, 2922–2930.
- (58) Thuo, M. M.; Martinez, R. V.; Liu, X.; Atkinson, M. B. J.; Bloch, J. F.; Whitesides, G. M. *Chem. Mater.* **2014**, *26*, 4260–4237.
- (59) Linder, V.; Sia, S. K.; Whitesides, G. M. *Anal. Chem.* **2005**, *77*, 64–71.
- (60) Chin, C. D.; Laksanasopin, T.; Cheung, Y. K.; Steinmiller, D.; Linder, V.; Parsa, H.; Wang, J.; Moore, H.; Rouse, R.; Umvilighozo, G.; Karita, E.; Mwambarangwe, L.; Braunstein, S. L.; van de Wiggert, J.; Sahabo, R.; Justman, J. E.; El-Sadr, W.; Sia, S. K. *Nat. Med.* **2011**, *17*, 1015–1019.
- (61) Disch, A.; Mueller, C.; Reinecke, H. *Conf. Proc. IEEE Eng. Med. Biol. Soc.* **2007**, 6322–6325.
- (62) Focke, M.; Kosse, D.; Muller, C.; Reinecke, H.; Zengerle, R.; von Stetten, F. *Lab Chip* **2010**, *10*, 1365–1386.